HHS Public Access

Author manuscript

Oncogene. Author manuscript; available in PMC 2012 November 17.

Published in final edited form as:

Oncogene. 2012 May 17; 31(20): 2566–2579. doi:10.1038/onc.2011.432.

F box protein FBXL2 exerts human lung tumor suppressor-like activity by ubiquitin-mediated degradation of cyclin D3 resulting in cell cycle arrest

Bill B. Chen[*,+], **Jennifer R. Glasser**[*,+], **Tiffany A. Coon**[*,+], and **Rama K. Mallampalli**[*,+,=,=]

[*]Department of Medicine, the University of Pittsburgh, Pittsburgh, PA 15213 USA

[+]Department of Acute Lung Injury Center of Excellence, the University of Pittsburgh, Pittsburgh, PA 15213 USA

[=]Department of Cell Biology and Physiology, the University of Pittsburgh, Pittsburgh, PA 15213 USA

[=]Medical Specialty Service Line, Veterans Affairs Pittsburgh Healthcare System

Abstract

Dyregulated behavior of cell cycle proteins and their control by ubiquitin E3 ligases is an emerging theme in human lung cancer. Here we identified and characterized the activity of a novel F box protein, termed FBXL2, belonging to the SCF (Skip-Cullin1-F-box protein) E3 ligase family. Ectopically expressed FBXL2 triggered G2/M phase arrest, induced chromosomal anomalies, and increased apoptosis of transformed lung epithelia by mediating polyubiquitination and degradation of the mitotic regulator, cyclin D3. Unlike other F box proteins that target phosphodegrons within substrates, FBXL2 uniquely recognizes a canonical calmodulin-binding motif within cyclin D3 to facilitate its polyubiquitination. Calmodulin bound and protected cyclin D3 from FBXL2 by direct intermolecular competition with the F box protein for access within this motif. The chemotherapeutic agent vinorelbine increased apoptosis of human lung carcinoma cells by inducing FBXL2 expression and cyclin D3 degradation, an effect accentuated by calmodulin knockdown. Depletion of endogenous FBXL2 stabilized cyclin D3 levels, accellerated cancer cell growth, and increased cell viability after vinorelbine treatment. Last, ectopic expression of FBXL2 significantly inhibited the growth and migration of tumorogenic cells and tumor formation in athymic nude mice. These observations implicate SCF^{FBXL2} as an indispensible regulator of mitosis that serves as a tumor suppressor.

Keywords

ubiquitin; camodulin; lung

Address Correspondence to: Rama K. Mallampalli, M.D. The University of Pittsburgh Pulmonary, Allergy, & Critical Care Medicine, UPMC Montefiore, NW 628 Department of Medicine Pittsburgh, PA 15213 Tel.: 412-692-2112 Fax: 412-692-2260 mallampallirk@upmc.edu.

INTRODUCTION

Lung cancer remains the leading cause of cancer deaths globally among men and women and yet novel and selective metabolic targets for therapeutic intervention in this illness require further study (Weiderpass 2010). The high proliferative capacity of lung neoplastic cells appears to be strongly linked to abberant regulation through critical checkpoints involved in cell cycle progression. D-type cyclins play integral roles in G1/S cell cycle progression (1995). Specifically, D type cyclins function through four cyclin-dependent kinases (Cdks): Cdk 2, Cdk 4, Cdk 5, and Cdk 6. Active cyclin D/Cdk 4 and cyclin D/Cdk 6 partially phosphorylate retinoblastoma tumor suppressor protein (Rb) thereby reducing its binding to E2F, and thus promoting cell progression to the S-phase by allowing E2F-mediated activation of cyclin E gene transcription (Ohtani et al 1995, Peeper et al 1997). There are three major cyclin D family members: cyclin D1, cyclin D2 and cyclin D3 of which cyclin D1 has been well studied (Lew et al 1991). As an important regulator for G1 to S phase progression, cyclin D1 plays an important role in multi-organ tumorogenesis (Gautschi et al 2007, Myung et al 2006, Zhang et al 2005, Zi and Agarwal 1999). Cyclin D1 degradation directly results in G1 phase arrest and thus might serve as a potential therapeutic target in neoplasia (Shan et al 2009).

Cyclin D1 is degraded mainly through its site-specific ubiquitination and disposal by the proteasome. Specifically, the SCF (Skp1-Cullin1-F-box) E3 ligase family members FBXO4, FBXW8, and FBXO31 directly interact with cyclin D1 and mediate its ubiquitination (Lin et al 2006, Okabe et al 2006, Santra et al 2009). However, more limited data are available regarding the function and molecular regulation of cyclin D3. Aside from its role in binding Cdk4 and Cdk6 to control G1 to S phase transition, cyclin D3 may have other functions in cellular division and intracellular signaling (Tanguay et al 2001). Cyclin D3 is ubiquitously expressed in several cell types, and also plays a role during the G2/M phase by interacting with CDK11p58 kinase during cell cycle progression. CDK11p58 promotes centrosome maturation and bipolar spindle formation and its interaction with cyclin D3 preserves CDK11p58 activity. Thus, the cyclin D3-CDK11p58 interaction appears to be vital during mitosis and its abrogation could lead to G2 arrest (Duan et al 2010, Zhang et al 2002). Moreover, some studies associate cyclin D3 with metastasis of nonsmall cell lung carcinoma and with reduced survival (Papay et al 2007, Sterlacci et al 2010).

Ubiquitination of proteins brands them for degradation either by the proteasome or via the lysosome that regulates diverse processes (Tanaka et al 2008). The conjugation of ubiquitin to a target protein is orchestrated by a series of enzymatic reactions involving an E1 ubiquitin-activating enzyme, ubiquitin transfer from an E1-activating enzyme to an E2-conjugating enzyme, and last, generation of an isopeptide bond between the substrate's ε-amino lysine and the carboxyl-terminus of ubiquitin catalyzed by a E3-ubiquitin ligase(Hochstrasser 2000). Of the many E3 ligases, the SCF superfamily is among the best studied (Tyers and Willems 1999). The SCF complex has a catalytic core complex consisting of Skp1, Cullin1, and the E2 ubiquitin-conjugating (Ubc) enzyme (Cardozo and Pagano 2004, Zheng et al 2002). The SCF complex also contains an adaptor receptor subunit, termed F-box protein, that target hundreds of substrates through phosphospecific domain interactions (Cenciarelli et al 1999). F-box proteins have two domains: an NH_2-

terminal F-box motif and a carboxyl-terminal leucine-rich repeat (LRR) motif or WD repeat motif. The SCF complex uses the F-box motif to bind Skp1, whereas the leucine-rich/WD repeat motif is used for substrate recognition (Ilyin et al 1999). Of the nearly 70 F-box proteins described, only ~ 6 have defined roles in cellular processes (Skaar et al 2009). Of note, the gene encoding the orphan F box protein, FBXL2, was strongly repressed in human lung adenocarcinoma (Malard et al 2007). Following its initial description (Ilyin et al 1999), FBXL2 was shown to interact with the hepatitis C virus nonstructural protein 5A (NS5A), and this association was required for viral RNA replication (Wang et al 2005). NS5A, and the lipogenic enzyme, cytidylyltransferase, are the only known targets of FBXL2 and its effects within the cell cycle pathway has not been investigated (Chen et al 2011).

Calmodulin (CaM) (16.7kD) is a highly conserved calcium-sensing protein that antagonizes some proteinases and modulates stability of regulatory proteins (Rhoads and Friedberg 1997). CaM binds its targets in a calcium bound (holoCaM) or calcium-1 free (apopCaM) form and thus its interactions with partners may be calcium -dependent or calcium -independent (Rhoads and Friedberg 1997). Many CaM binding proteins harbor recognition motifs characterized by a basic amphipathic helix, moderate to high helical hydrophobic moment, and a net positive charge. Other motifs described include an IQ motif (I/LQXXXRGXXXR), a 1-8-14, and 1-5-10 CaM binding motif (Rhoads and Friedberg 1997). As a major intracellular calcium receptor, CaM exerts multiple modes of regulatory control within the cell cycle (Kahl and Means 2003). For example, CaM appears essential for cyclin-dependent kinase 4 (Cdk4) activity and nuclear accumulation of cyclin D1-Cdk4 during the G1 phase (Taules et al 1998). CaM also binds to the centrosome protein CP110, and CaM RNAi impairs the latter stages of cytokinesis leading to the formation of binucleate cells (Tsang et al 2006). Interestingly, CaM also directly interacts with cyclin E and mediates calcium sensitive G1/S phase transition (Choi et al 2006, Choi and Husain 2006). We showed that CaM binds and stabilizes cytidylyltransferase required for phospholipid synthesis during cellular membrane formation suggesting that its combinatorial effects regulate processes intrinsic to cellular growth and repair (Chen and Mallampalli 2007).

Here, by using a SV40-tumorogenic cell line (Wikenheiser et al 1992), we show that cyclin D3 is polyubiquitinated by FBXL2 and degraded within the proteasome, and that this process is attenuated by CaM. Cyclin D3 stability is not controlled by FBXL2 targeting of a phosphodegron typical of F box proteins. Rather, FBXL2 recognizes and binds in a calcium-independent manner to an IQ molecular signature also recognized by CaM. SCF^{FBXL2} mediated cyclin D3 ubiquitination and degradation was sufficient to induce mitotic arrest in the SV40 transformed cell line and inhibited growth of human adenocarcinoma xenografts in nude mice indicative of ability of this orphan F box protein to exert anti-tumor activity.

RESULTS

Ectopic expression of FBXL2 induces G2 arrest and degradation of cyclin D3

We investigated FBXL2 activity on cell cycle progression first using a transformed murine lung epithelial (MLE) cell line and then extended studies to use of human adenocarcinoma cells. Overexpression of FBXL2, unlike mutant FBXL2 (N100) lacking its F-box domain,

results in accumulation of rounded, apoptotic cells (Fig. 1A). These morphological changes after ectopic expression of FBXL2 were associated with cell cycle arrest, as evidenced by reduced DNA synthesis and a significant increase in a cell population within the G2/M phase that accumulated in a time-dependent manner (Fig. 1B, Fig. S1). To investigate the mechanism by which FBXL2 induced G2/M arrest, we analyzed immunoreactive levels of fifteen cell cycle regulatory proteins after FBXL2 overexpression. Surprisingly, we observed that the levels of cyclin D2 and cyclin D3, two G1/S phase regulators, markedly decreased (Fig. 1C). In contrast, levels of other G1 cyclins and the G2/M regulators cyclin A and cyclin B were unaffected. Ectopic FBXL2 expression did not alter levels of other Cdks or negative control proteins, but did decrease levels of a known substrate, CCT (Chen et al 2011). Of note, ectopic expression of dominant negative mutant FBXL2N100 modestly increased immunoreactive cyclin D2 and cyclin D3 levels (Fig. S2). RNAi-mediated knockdown of cyclin D3, but not cyclin D2, reproduced in part, effects of FBXL2 overexpression with regard to G2 arrest in cells (Fig. 1D, and Fig. S3). Cyclin D3 silencing resulted in significant increases (~50%) in the G2 phase, whereas knockdown of cyclin D2 showed limited effects (Fig. S4A). Knockdown of cyclin D3, but not cyclin D2, promotes apoptosis (Fig. S4B). RNAi-mediated knockdown of FBXL2 had no effect on the G2-phase, but tended to increase the S-phase and reduced the G1 phase (Fig. S5). These results were somewhat marginal (~30%), but suggest that in MLE cells, cyclin D3 as a D-type cyclin also triggers G1-S phase progression. Alternatively, FBXL2 might exert a more complex effector role with other yet unidentified substrates during cell cycle progression, some of which may be required for S-phase entry or egress.

We next examined cyclin D3 half-life after FBXL2 overexpression and knockdown. Ectopic FBXL2 expression significantly decreased $t_{1/2}$ of cyclin D3, whereas knockdown of FBXL2 markedly increased cyclin D3 $t_{1/2}$ (Fig. 1E). Consistent with these results FBXL2 overexpression did not significantly alter CCND2 or CCND3 steady-state mRNA levels (Fig. S6). To further assess the specificity of these effects, a random F-box protein (FBXL12) from the FBXL family was selected and ectopically expressed in cells demonstrating lack of ability of this protein to disrupt cyclin D3 stability (Fig. S7). Moreover, loss and gain-of function studies of FBXL2 did not alter cyclin D1 $t_{1/2}$ (Fig. S8). Last, ectopic expression of FBXL2 results in a reduction in endogenous cyclin D2 and cyclin D3 levels in other cell lines (Fig. S9).

FBXL2 targets cyclin D3 for ubiquitination during mitosis

To test whether FBXL2 interacts with cyclin D3, we performed co-immunoprecipitation (co-i.p.) experiments. MLE cells were first synchronized separately to G1, S, and the G2 phase; mitotic cells were also collected through shake-off. Cells were immediately lysed and subjected to FBXL2 i.p. Cyclin D3 and FBXL2 immunoreactive levels oscillated during the cell cycle; low levels of endogenous cyclin D3 linked to high levels of FBXL2 tended to occur during mitosis (Fig 2A, left panel, and input, [M]). Also, cyclin D3 in the FBXL2 immunoprecipitates was only detected in mitotic cells (Fig. 2A). Thus, endogenous FBXL2 protein targets cyclin D3 during mitosis. When a panel of cells was immunostained for cyclin D3 and counterstained with DAPI to visualize the nucleus, the fluorescent intensity representing endogenous cyclin D3 levels was lower in identified cells undergoing mitosis

when compared to cells in interphase (Fig. 2B). In other experiments, synchronized cells were subjected to cyclin D3 co-i.p.; the immunoprecipitates were then resolved in SDS-PAGE and probed with ubiquitin. Polyubiquitinated products (a high molecular weight smear) of cyclin D3 were detected during mitosis (Fig. 2C, arrows). Hence, endogenous FBXL2 targets these cyclins for polyubiquitination not during interphase but with mitosis. We next determined the subcellular pathway for FBXL2-mediated degradation of cyclins. Addition of the proteasomal inhibitor, MG132, to cells led to accumulation of cyclin D3 protein whereas this was not seen with the lysosomal inhibitor, leupeptin (Fig. 2D). Importantly, inclusion of purified SCF^{FBXL2} with the full complement of E1 and E2 enzymes plus ubiquitin was sufficient to generate polyubiquitinated cyclin D3 species *in vitro* (Fig. 2E).

Cyclin D3 is polyubiquitinated within its C-terminus

To determine the ubiquitination acceptor site within cyclin D3, deletional and candidate approaches were used that suggested that Lys^{268} might be a functionally relevant molecular site (Fig. 3A, data not shown). Thus, we examined polyubiquitination and stability of a Lys^{268R} mutant in cells (Fig. 3B). MG132 treatment triggered appearance of polyubiquitinated wild-type cyclin D3; in contrast, the proteasomal inhibitor failed to increase accumulation of the cyclin D3 mutant, suggesting that Lys^{268} is a putative ubiquitination site for cyclin D3 (Fig. 3B). The Lys^{268R} mutant exhibited significantly extended $t_{1/2}$ compared to the wild-type cyclin (Fig. 3C). Co-expression of FBXL2 with cyclins resulted in the degradation of wild-type cyclin D3, but not the Lys^{268R} mutant mutant (Fig. 3D). Using *in vitro* ubiquitination assays in which wild-type or mutant cyclin D3 were reacted with the purified ubiquitin SCF^{FBXL2} complex, the Lys^{268R} mutant was not ubiquitinated (Fig. 3E). Importantly, after expression of mutant cyclin D3, ectopically expressed FBXL2 failed to induce efficient G2/M arrest (Fig. 3F).

FBXL2 and CaM both vie for cyclin D3 docking

Calmodulin binds and protects some regulatory proteins and is needed for cell cycle progression (Kahl and Means 2003). Cyclin D3 harbors two potential CaM binding IQ motifs within its NH_2-terminus suggesting that these motifs may be required for CaM interaction (Fig. 3A). Wild-type or NH_2-terminal deletion cyclin D3 were transfected in cells, cell lysates were then applied to CaM-sepharose beads to test protein interaction. The pull-down experiments show that only wild-type cyclin interacts with CaM optimally with inclusion of EDTA, and this interaction was significantly disrupted by even low micromolar calcium concentrations (Fig. 4A, top panel). A cyclin D3 variant devoid of the amino-terminus failed to interact with CaM, supporting the premise that an IQ motif within this region is required for molecular interaction between the cyclin D3 and CaM (Fig. 4A). We next identified which of the two potential IQ motifs within cyclin D3 are required for CaM binding. Glu^{100} of cyclin D3 was essential for CaM binding (Fig. 4A, lower panel). Interestingly, FBXL2 also failed to interact with the NH_2-terminal deletion cyclin D3 (Fig. 4B, top panel). Importantly, FBXL2 also utilizes this molecular site (Glu^{100}) within this motif to target cyclin D3 (Fig. 4B, lower panel). Co-expression of FBXL2 with cyclins resulted in the degradation of wild-type cyclin but not the cyclin $D3^{Q100A}$ point mutant and failed to induce efficient G2/M arrest (Fig. 4C,D). For confirmation, *in vitro* ubiquitination

assays demonstrated that the point mutant of cyclin D3 (Q100A) was not ubiquitinated (Fig. 4E), and this variant exhibited a significantly longer $t_{1/2}$ compared to wild-type cyclin D3 (Fig. 3F). FBXL family proteins contain leucine-rich repeats (LRR) for substrate targeting and residues 80–423 contain 12 LRRs that display extensive internal homology (Fig. 3G). In mapping studies, cell lysates expressing his-tagged FBXL2 truncation mutants were co-purified with GST-cyclin D3 using his-pull downs. The data show that deletion of the last five LLRs (C250) or the last two LLRs (C350) markedly disrupted FBXL2-cyclinD3 interaction. Thus, cyclin D3 binds FBXL2 within its last two LLR domains (350–423).

Cyclin D3 polyubiquitination is largely phosphorylation-independent

Traditional mechanisms of cyclin degradation appear to involve signals involving phosphorylation of Thr^{286} (Diehl et al 1997). To determine whether FBXL2:cyclin D3 interaction is phosphorylation-dependent, mitotic cell lysate from MLE cells was treated with either vehicle or phosphatase followed by coimmunoprecipitation of endogenous FBXL2. The results indicate that cyclin D3 associates with FBXL2 in both vehicle and phosphatase treated immunoprecipitated samples (Fig. S10A); thus, FBXL2 interaction with cyclin D3 is phosphorylation-independent. Similar results were observed in A549 cells (Fig. S10B). Further, both wild-type and phosphatase-treated cyclin D3 were prone to *in vitro* ubiquitination by FBXL2 (Fig. S11). Additional studies interrogated the corresponding T283 molecular site within cyclin D3. Both wild-type cyclin D3 and a cyclin D3 Thr^{283A} mutant bound FBXL2 and FBXL2 ubiquitinated both substrates *in vitro* (Fig. S12). Last, although the Thr^{283A} mutant displayed modestly extended protein t ½ compared to wild-type cyclin D3, only a double mutant ($Q100^{A}$ Thr^{283A}) exhibited significantly stability (Fig. S13). The results do not exclude cyclin D3 ubiquitination by other F box proteins, but suggest strongly that FBXL2 partakes in its turnover and that this involves an IQ motif.

SCF^{FBXL2} directed ubiquitination of cyclin D3 is antagonized by CaM

CaM overexpression significantly increased cyclin D3 half-life, whereas CaM knockdown decreased the stability of the protein (Fig. 5A). Similar to ectopic FBXL2 expression and CaM repression (Lu et al 1992), CaM silencing resulted in G2/M arrest, whereas overexpression of CaM increased the proportion of cells within the S-phase (Fig. 5B). CaM also directly interacts with FBXL2, as several bulky and hydrophobic residues within the F-box amino-terminus appear important for CaM interaction (data not shown). We next tested the functionality of mutant FBXL2 proteins. Cells transfected with either wild-type FBXL2 or $FBXL2^{F79A}$ (that does not bind CaM, data not shown) effectively decreased cyclin levels (Fig. 5C, left panel) and resulted in G2/M arrest (Fig. 5D). When cells were pre-infected with a replication-deficient adenovirus expressing CaM (Adv-CaM) and then transfected with these FBXL2 plasmids, CaM gene transfer was not able to totally rescue cyclin D3 protein levels (Fig. 5C right panel), nor prevent G2/M arrest when cells were transfected with $FBXL2^{F79A}$ (Fig. 5D). These results suggest that in addition to competition for IQ motif occupancy within cyclins, CaM's ability to directly bind and sequester FBXL2 to protect cyclin D3 might also be functionally important.

We also investigated the FBXL2, CaM, and cyclin interactions during cell cycle progression. Lysate from synchronized cells were subjected to FBXL2, cyclin D3 i.p., the

immunoprecipitates were then resolved in SDS-PAGE and probed with CaM. There was significant loss of FBXL2/CaM binding during mitosis and CaM associates with cyclin D3 at the highest levels during the S-phase with limited, if any, binding during mitosis (Fig. 5E). Since both CaM and FBXL2 interact with cyclins through the same IQ motif, we next tested the concept that there exists intermolecular competition between FBXL2 and CaM for cyclin D3 binding. This was analyzed using pull-down experiments in the presence or absence of calcium in which FBXL2 was immobilized on beads and used as bait for cyclins and CaM (Fig. 5F). Three negative controls were included: 1) FBXL2-agarose alone was assayed to control for cyclin and CaM contamination; 2) Cyclin D3 and CaM with calcium were run over empty talon beads, eluted, and proteins were resolved by SDS-PAGE followed by cyclin and CaM immunoblotting to ensure that associations were FBXL2 specific; and 3) V5 immunoblotting was used as a loading control, to ensure that pull-down experiments had equivalent amounts of FBXL2. The results indicate that not only does FBXL2 directly interact with cyclin D3 and CaM, but that excess CaM disrupts FBXL2 interaction with cyclin D3 (Fig. 5F). Interestingly, excess calcium promotes cyclin D3 binding to FBXL2. By using a synthetic cyclin D3 peptide (LQLLGTVCLL) encoding the putative CaM-binding motif, we observed tight binding between CaM and cyclin D3 (K_d= 0.31 μM, Fig. 5G) using isothermal calorimetry.

Ectopic expression of FBXL2 induces apoptosis

Ectopic expression of FBXL2 triggered an increase in apoptosis in human lung adenocarcinoma (A549) cells by FACS analysis using annexin V staining (Fig. 6A,B). Viable cells were also quantified (Fig. 6C), showing that FBXL2 markedly inhibited the growth of A549 cells in culture. A549 cells transfected with siRNA targeting CaM or FBXL2 also displayed differential cell numbers, as FBXL2 knockdown promoted growth of A549 cells in culture, consistent with ability of FBXL2 knockdown to increase S-phase (Fig. S5). We further tested ability of lung cancer chemotherapeutic agents to induce FBXL2 levels. Of the agents examined, only vinorelbine, a drug that causes G2/M arrest in lung cancer, increased FBXL2 levels and decreased cyclin D3 content (Fig. 6E). The kinetics of vinorelbine effects revealed that by 15 h sufficient induction of FBXL2 and decreased levels of cyclin D3 were observed (Fig. 6F). A549 cells were also transfected with siRNA against FBXL2 or CaM for 48 h, before exposure to vinorelbine for additional 48 h. Apoptosis was measured by FACS analysis using annexin V staining (Fig. 6G) and quantified in (Fig. 6H). The results demonstrate that CaM knockdown accentuated, whereas FBXL2 silencing reduced A549 cells apoptosis induced by vinorelbine.

Ectopic expression of FBXL2 inhibits tumorogenicity

Initially, we assessed tumor cell migration using a would-healing assay. FBLX2 overexpression inhibited A549 cell migration, whereas co-expression of a proteolytically resistant cyclin D3 was able to restore cell migratory activity (Fig. 7A). We also transfected A549 cells with a plasmid encoding doxycycline-inducible FBXL2. Doxycycline increased levels of immunoreactive FBXL2 that in turn induced cyclin D3 degradation coupled with an increase in cellular apoptosis (Fig. 7B). As a complementary *in vivo* model, we assessed tumorogenicity after implanting A549 cells under either stable or inducible expression of FBXL2 in athymic nude mice. Stable expression of FBXL2 significantly reduced tumor size

compared to the control implants (Fig. 7C). Similar results were also obtained by using the inducible system for FBXL2 expression (Fig. S14). Importantly, when tumor tissues were collected from four control and four FBXL2 mice at the end-point and analyzed, immunoblotting showed significant decreases in cyclin D3 protein levels coupled with increased levels of FBXL2 protein (Fig. 7D).

DISCUSSION

The precise role of the majority SCF-based E3 ligases, including F box proteins, has not been established. The observation that FBXL2 is repressed in human lung adenocarcinoma (Malard et al 2007) raises the possibility that it might regulate molecular programs involved in neoplasia, such as cell cycle progression. Here, we show that both ectopically expressed and endogenous FBXL2 regulate viablity and proliferation of transformed or tumorogenic epithelia by ubiquitin-mediated degradion of cyclin D3. We also observe opposing activities of SCF^{FBXL2} and a ubiquitous calcium sensor, CaM, on cyclin D3 polyubiquitination and degradation. FBXL2 functions as the receptor component of a prototypical SCF ubiquitin E3 ligase that targets a CaM binding signature; this represents a unique property of FBXL2 as other F-Box proteins recognize phosphoserine or phosphothreonine sites within target substrates (Hansen et al 2004, Liu et al 1999, Watanabe et al 2005). For example, the well-studied family member cyclin D1 harbors a key site (Thr^{286}) for recognition by the E3 ligase subunits FBXO4, FBXW8, and FBXO31 (Lin et al 2006, Okabe et al 2006, Santra et al 2009). Although this Thr site is conserved among the D cyclins and might also be used as a targeting signal by cyclin D3 for other F box proteins, FBXL2 did not utilize this signature for its substrate. This was evidenced by the ability of both dephosphorylated cyclin D3 and a related point mutant (cyclin $D3^{T283A}$) to bind and be ubiquitinated by FBXL2 (Figs. S10–S12). Rather, FBXL2 docks within a consenus IQ signature within its substrate to facilitate ubiquitination. This was evidenced by ectopic expression of point mutants of cyclin D3 within the IQ motif that were resistant to ubiquitination and were sufficient to extend cyclin D3 half-life (Fig. 4F). Whether FBXL2 uses this mode of targeting to other substrates requires additional investigation, but these results provide the first evidence that this F-box protein appears to be a major regulator of cyclin D3 lifespan and thus might serve as a key growth inhibitory signal.

F-box protein mediated ubiquitination and proteasomal degradation of cyclin D3 resulting in G2/M arrest was unexpected, as these cyclins predominantly regulate G1/S transition and knockdown of cyclin D3 has been shown to induce G1 arrest (Sicinska et al 2003). However, cyclin D3 may have a dual role in also mediating G2/M phase progression (Fang et al 2002, Zhang et al 2002). Thus, in lymphoblastic cells that selectively and highly expressed cyclin D3, its knockdown was expected to result in G1 arrest given the role of D-type cyclins in G1-S progression. However, in our studies, MLE cells express all three D-type cyclins, and overexpression of FBXL2 selectively down-regulated cyclin D3, but not cyclin D1; hence because of cyclin D redundancy G1/S phase progression is preserved and G2/M arrest was observed. In addition to this redundancy, the G1/S phase may also be less prone to FBXL2-induced blockade because of lower FBXL2 levels during interphase and higher levels of CaM and cyclin D3.

As above, cyclin D3 is also a multi-functional protein that directly interacts with and confers activity for CDK11p58 (Duan et al 2010, Zhang et al 2002), a key cyclin-dependent kinase that controls centrosome maturation and bipolar spindle formation (Petretti et al 2006). As with ectopic FBXL2 in cells, knockdown of CDK11p58 results in G2 arrest and apoptosis; significant CDK11 depletion results in misaligned and lagging chromosomes, permanent mitotic arrest, and cell death (Hu et al 2007). Hence, SCF^{FBXL2} directed ubiquitination and degradation of cyclin D3 would potentially impair its association with CDK11p58 and reduce its activity. One additional function of CDK11 is to recruit Polo-like kinase 4 (PLK4) and Aurora A to the centrosome that also regulate mitotic events and chromosomal stability (Petretti et al 2006). Knockout of PLK4 or expression of a defective mutant Aurora protein also results in apoptosis (Rosario et al 2010) (Glover et al 1995). Collectively, these results suggest that one explanation for G2/M phase delay and apoptosis might involve SCF^{FBXL2} inactivation of CDK11p58 by ubiquitination and depletion of cyclin D3. This mechanism would dislocate PLK4 and Aurora A causing cell cycle arrest (Fig. 8). In support of this, ectopic expression of FBXL2 does not decrease CDK11 protein levels but reduces assembly of the cyclin D3: CDK11p58 complex and binding of PLK4 and Aurora A (data not shown). There also exist some differing effects on cycle progression after silencing cyclin D2 or cyclin D3. Knockdown of cyclin D3, but not cyclin D2, resulted in G2/M arrest. Because both cyclins are highly conserved and exert some redundant functions, a more modest phenotype observed with cyclin D2 knockdown might be because of compensation by cyclin D3. This would occur especially if lower levels of cyclin D2 are present in MLE cells compared to cyclin D3 as seen with A549 cells and CHO cells (Fig. S9).

We have uncovered functionally distinct domains that govern molecular interplay between the effectors, FBXL2 and CaM, and their putative targets, cyclin D3. First, cyclin D3 harbors a canonical IQ motif typical of calcium independent CaM binding proteins (Fig. 4A). Accordingly, both FBXL2 and CaM target this signature within cyclin D3 and bind in the absence of calcium (Fig. 4A, 5E). Structural analysis predicts a α-helix for the IQ signature with cyclin D3 (LQLLGTVCLL). Interestingly, cyclin D1 contains a modified sequence (LQLLGATCMF) with substitution of a Thr for a hydrophobic residue at position seven. This could explain our findings that ectopic expression or knockdown of FBXL2 does not affect cyclin D1 levels (Fig. S8). Alternatively, this could be because cyclin D3 is the dominant D-type cyclin within the MLE cells, thus prone to FBXL2 targeting.

Our data indicate that calcium availability differentially regulates the interactions between the F box protein, CaM, and the FBXL2 substrate. In our prior studies, the presence of calcium did not alter the molecular interaction between CaM and cytidylyltransferase (Chen and Mallampalli 2007) and yet CaM binding with cyclin D3 was completely interrupted by even 1 μM calcium. In both cases calcium promotes FBXL2 interaction with its substrates, although FBXL2 still associates with cyclin D3 in the absence of calcium. Physiologically, these molecular interactions might depend upon subcellular compartmentalization of binding partners and availability of calcium signals within these compartments. For example, cytidylyltransferase is an amphitrophic enzyme that largely exists in the cytoplasm in lung cells whereas cyclins are nuclear (Ridsdale et al 2001). Hence, cytidylyltransferase would be predicted to be protected by CaM in settings when calcium levels are very low, but during sepsis when cytosolic calcium currents fluctuate, it might be prone to ubiquitination by

calcium-activated SCF^{FBXL2} (Chen et al 2011). In the nucleus, the physiological levels of calcium will also likely regulate these molecular interactions during cell division. Although cyclin D3 binds CaM in the absence of calcium, a modest increase in calcium (~1000nM) almost totally disrupts cyclin D interaction with CaM (Fig. 4A, 5E) and calcium increases cyclin D3 binding to FBXL2 (Fig. 5F). However, during the G1/S phase, CaM binds cyclin D3 (Fig. 5E) when low levels of calcium (20–40 nM) are typically present in the nucleus providing an environment conducive for these interactions (Korkotian and Segal 1996). Moreover, during prophase the nuclear envelope is disrupted, chromosomal condensation occurs, and nuclear contents are transiently exposed to higher calcium concentrations within the cytosol (200–1000 nM) (Brown and Shoback 1984, Pszczolkowski et al 1999). The prediction is that these higher calcium concentrations would trigger CaM dissociation from cyclin D3 to enhance cyclin vulnerablity for SCF^{FBXL2} mediated ubiquitination. Here, calcium might play a more important role in destabilizing cyclin D3 by releasing CaM and recruiting SCF^{FBXL2} to the IQ motif.

Our data suggest that cyclin D3 availability required for cell cycle progression will also depend on the relative binding affinities between FBXL2, CaM, and their targets. Each of these proteins was demonstrated to interact *in vitro* (Fig. 5F). Of note, despite ectopic expression of an Adv5-CaM in cells, this was inefficient at restoring cyclin D3 levels when co-expressing an FBXL2 mutant that lacks ability to interact with CaM. These results suggest that CaM's ability to act as a decoy to directly antagonize and sequester the F-box protein represents a mechanistically relevant interaction in addition to FBXL2 and CaM intermolecular competition for occupancy within the cyclin IQ motif. However, our isothermal calorimetry studies demonstrating very low binding constants between CaM and cyclin D3 (K_d= 0.31 μM, (Fig. 5G)) versus relatively higher values between CaM and FBXL2 (K_d= 0.81 μM, data not shown) suggest that CaM competition with FBXL2 might be a more functionally relevant mechanism *in vivo*.

The data presented here suggest that tight interplay between F-box protein FBXL2 and CaM will regulate mitotic events through control of cyclin D3 abundance. CaM plays a vital role in centrosome formation during mitosis by interacting with the centrosome protein, CP110; mutant CP110 that lacks ability to bind CaM leads to failure of cytokinesis (Tsang et al 2006). Counter-intuitively, CaM fails to protect cyclin D3 during mitosis thereby potentially contributing to SCF^{FBXL2}-induced ubiquitination and degradation. As stated above, cyclin D3 dependent CDK11p58 activity is also essential for mitosis, but excessive CDK11p58 levels repress cellular proliferation and induce apoptosis (Duan et al 2010). Hence, the dissociation of CaM from cyclin D3 and its targeting by the SCF^{FBXL2} complex during the transition to mitosis might be an exquisite mechanism to balance CDK11p58 levels thereby regulating cell proliferation.

MATERIALS AND METHODS

Materials

The sources of the transformed murine lung epithelial (MLE) cell line, CaM, Erk, LPCAT1, and GST antibodies were described previously (Chen and Mallampalli 2007, Ray et al 2010). Purified SCF^{FBXL2} was purchased from Abnova (Walnut, CA). Purified bovine

calmodulin, ubiquitin, E1, E2, MG132, leupeptin, and cycloheximide were purchased from Calbiochem (La Jolla, CA). Rabbit polyclonal ubiquitin, cyclin and Cdk sampler kits, were purchased from Cell Signaling (Danvers, MA). Mouse monoclonal cyclin D2 and cyclin D3 antibodies were from Abcam (Cambridge, MA). Doxycycline, were purchased from Clontech (Mountain view, CA). Lipofectamine 2000, mouse monoclonal V5 antibody, DAPI nuclear staining kits, the pcDNA3.1D cloning kit, *E. coli* One Shot competent cells, the pENTR Directional TOPO cloning kits, and the Gateway mammalian expression system were from Invitrogen (Carlsbad, CA). BD TALON purification and buffer kits, and FACS kit were purchased from BD Biosciences (San Jose, CA). The F-box proteins cDNA were purchased from OpenBiosystems (Huntsville, AL). Nucleofector transfection kits were from Amaxa (Gaithersbury, MD). Adenoviral constructs encoding CaM were generated as described (Chen and Mallampalli 2007). Immobilized protein A/G beads were from Pierce (Rockford, IL). Cell viability based on ATP generation was assayed using a CellTiter-Glo® Luminescent Cell Viability kit from Promega, (Madison, WI). Annexin V staining kits and the complete proteasome inhibitors were from Roche (Madison, WI). Lambda protein phosphatase was from New England Biolabs (Ipswich, MA). Goat polyclonal FBXL2 antibody, scrambled RNA, and siRNAs were from Santa Cruz Biotechnology (Santa Cruz, CA). Rabbit polyclonal FBXL2 antibody was custom made from Rockland Immunochemicals Inc (Gilbertsville, PA). All DNA sequencing was performed by the University of Pittsburgh DNA Core Facility.

Cell culture

MLE cells were cultured in Dulbecco's Modified Eagle Medium-F12 (Gibco) supplemented with 2–10% fetal bovine serum (DMEM-2 or 10). Cells in some studies were synchronized using serum starvation (DMEM-F12) for 48 h or treatment with nocodazole or aphidicolin. In other studies, cells were treated with leupeptin or MG132 at 1:2000 dilution. For half-life studies, cells were treated with cycloheximide (40 μg/ml) at different time points. Cells lysates were prepared by brief sonication in 150 mM NaCl, 50 mM Tris, 1.0 mM EDTA, 2 mM dithiothreitol, 0.025% sodium azide, and 1 mM phenylmethylsulfonyl fluoride (Buffer A) at 4 °C.

Expression of recombinant protein and RNAi

All plasmids were delivered into cells using nucleofection or lipofectamine 2000 (Agassandian et al 2010, Chen and Mallampalli 2009). Cellular expression of green fluorescent tagged plasmids using this device was achieved at >90%. For overexpression of CaM, 4×10^6 cells were plated in 100 mm dishes for 24 h, then infected with Adv-CaM or an empty vector (Adv-Con) at MOI=40 for 12 h followed by FBXL2 plasmid expression. For siRNA studies, 1×10^6 cells were transfected using lipofectamine 2000 with 10 μg of RNA and harvested after an additional 48 h.

Co-immunoprecipitation and binding assays

*25*0 μg of total protein from cell lysates was precleared with 20 μl of protein A/G beads for 1 h at 4 °C. 5 μg of primary antibody was added for 18 h incubation at 4°C. 40μl of protein A/G beads were added for an additional 6 h of incubation. Beads were slowly centrifuged

and washed five times using 50 mM HEPES, 150 mM NaCl, 0.5 mM EGTA, 50 mM NaF, 10 mM Na_3VO_4, 1 mM phenylmethylsulfonyl fluoride, 20 μM leupeptin, and 1% (v/v) Triton X-100 (RIPA) buffer, as described (Mallampalli et al 2000). The beads were heated at 100 °C for 5 min. with 80 μl of protein sample buffer prior to SDS-PAGE and immunoblotting. For CaM binding assays, CaM sepharose beads were incubated with V5-FBXL2 or cyclin D3 transfected cell lysates (50 μg), with or without Ca^{2+} at 4°C for 2 h. Eluted products were processed for SDS-PAGE and immunoblotting as described (Chen and Mallampalli 2007).

Immunostaining

Cells (2×10^5) were plated at 70% confluence on 35mm MetTek glass bottom culture dishes. Immunofluorescent cell imaging was performed on a Nikon A1 confocal microscope using 405 nm, 458 nm, 488 nm, 514 nm or 647 nm wavelengths. All experiments were done with a 60 × oil differential interference contrast objective lens. Cells were washed with PBS and fixed with 4% paraformaldehyde for 20 min, then exposed to 15% BSA, 1:500 primary antibodies, and 1:1000 Alexa 488 or Alexa 647 labeled goat anti-mouse or rabbit secondary antibody sequentially for immunostaining.

In vitro ubiquitin conjugation assay

The ubiquitination of V5-cyclin D3 was performed in a volume of 25 μl containing 50 mM Tris pH 7.6, 5 mM $MgCl_2$, 0.6 mM DTT, 2 mM ATP, 1.5 ng/μl E1, 10 ng/μl Ubc5, 10 ng/μl Ubc7, 1μg/μl ubiquitin (Calbiochem), 1 μM ubiquitin aldehyde, 4–16 μl of purified Cullin1, Skp1, Rbx1, and *in vitro* synthesized FBXL2. Reaction products were processed for V5 immunoblotting.

Quantitative RT–PCR, cloning, and mutagenesis

Total RNA was isolated and reverse transcription was performed followed by quantitative real-time PCR with SYBR Green qPCR mixture as described (Butler and Mallampalli 2010). All mutant constructs were generated using PCR-based approaches using appropriate primers or site-directed mutagenesis. PCR based approaches were used to clone FBXL2 into Plvx and Plvx-Tight vectors (Clontech) for constitutive or inducible expression of FBXL2 in A549 cells. To generate lentivirus encoding FBXL2, Plvx-FBXL2, Plvx-Tight-FBXL2, Plvx-TetOn plasmids were co-transfected with Lenti-X HTX packaging plasmids into 293FT cells following the manufacturers' instructions. 72 h later, virus was collected and titered using a p24 Rapid Titration Kit (Clontech). A549 cells were either infected with lentivirus encoding Plvx-FBXL2 for constitutive FBXL2 expression or infected with lentivirus encoding Plvx-Tight-FBXL2 and Plvx-TetOn for inducible FBXL2 expression.

Cell cycle and apoptosis analysis

Transfected cells were incubated with BrdU (20 μM) for 40 min, fixed, and stained following manufacturer's protocols (BD Biosciences, Sparks, MD). FACS samples were analyzed with the AccuriC6 system. DNA content was analyzed using FCS3 express software (De Novo Software, Los Angeles, CA). When analyzing cell cycle, a gate for 7AAD was set to exclude polyploidy cells. Otherwise cells were counted and the percentage

of cells with 2N, 4N and 8N DNA content was expressed as a percentage of total cells. Cells were also stained with annexin V for 15 min following the manufacturer's protocol (Roche). Apoptotic cells were counted, and apoptotic cells were expressed as a percentage of total cells.

Cell migration assays

A549 cells were plated in 6-well plates followed by transfection of the plasmids. 24 h later, a thin line was created on the cell monolayers by scratching using a pipet tip. Cells were observed under light microscopy and photos taken over time and migratory activity representative of three individual wells was analyzed by imageJ software.

Animal studies

Nude/Nude mice (purchased from Charles River) were acclimated at the University of Pittsburgh Animal Care Facility and maintained according to all federal guidelines and under the University of Pittsburgh Institutional Animal Care and Use Committee (IACUC) approved protocols. Mice were deeply anesthetized with ketamine (80–100 mg/kg intraperitoneally (i.p.) and xylazine (10 mg/kg i.p.), followed by i.p. injection of 5×10^6 A549 cells (100μl) into the left shoulder. To induce FBXL2 expression, 2 mg/ml of doxycycline was added to the drinking water. Mice were closely monitored every three days; tumor volume was calculated using a formula length×width×height× $\pi/6$.

Statistical Analysis

Statistical comparisons were performed with the Prism program, version 4.03 (GraphPad Software, Inc., San Diego, CA) using an ANOVA 1 or an unpaired 2 t-test with $p<0.05$ indicative of significance.

Supplementary Material

Refer to Web version on PubMed Central for supplementary material.

ACKNOWLEDGMENTS

We thank A.F. Stewart for critical review of the manuscript and helpful suggestions. This material is based upon work supported, in part, by the US Department of Veterans Affairs, Veterans Health Administration, Office of Research and Development, Biomedical Laboratory Research and Development. This work was supported by a Merit Review Award from the US Department of Veterans Affairs and National Institutes of Health R01 grants HL096376, HL097376 and HL098174 (to R.K.M.). The contents presented do not represent the views of the Department of Veterans Affairs or the United States Government.

REFERENCES

Agassandian M, Chen BB, Schuster CC, Houtman JC, Mallampalli RK. 14-3-3zeta escorts CCTalpha for calcium-activated nuclear import in lung epithelia. FASEB J. 2010; 24:1271–1283. [PubMed: 20007511]

Brown EM, Shoback DM. The relationship between PTH secretion and cytosolic calcium concentration in bovine parathyroid cells. Prog Clin Biol Res. 1984; 168:139–144. [PubMed: 6096881]

Butler PL, Mallampalli RK. Cross-talk between remodeling and de novo pathways maintains phospholipid balance through ubiquitination. J Biol Chem. 2010; 285:6246–6258. [PubMed: 20018880]

Cardozo T, Pagano M. The SCF ubiquitin ligase: insights into a molecular machine. Nat Rev Mol Cell Biol. 2004; 5:739–751. [PubMed: 15340381]

Cenciarelli C, Chiaur DS, Guardavaccaro D, Parks W, Vidal M, Pagano M. Identification of a family of human F-box proteins. Curr Biol. 1999; 9:1177–1179. [PubMed: 10531035]

Chen BB, Mallampalli RK. Calmodulin binds and stabilizes the regulatory enzyme, CTP: phosphocholine cytidylyltransferase. J Biol Chem. 2007; 282:33494–33506. [PubMed: 17804406]

Chen BB, Mallampalli RK. Masking of a nuclear signal motif by monoubiquitination leads to mislocalization and degradation of the regulatory enzyme cytidylyltransferase. Mol Cell Biol. 2009; 29:3062–3075. [PubMed: 19332566]

Chen BB, Coon TA, Glasser JR, Mallampalli RK. Calmodulin antagonizes a calcium-activated SCF ubiquitin E3 ligase subunit, FBXL2, to regulate surfactant homeostasis. Mol Cell Biol. 2011; 22:22.

Choi J, Chiang A, Taulier N, Gros R, Pirani A, Husain M. A calmodulin-binding site on cyclin E mediates Ca2+-sensitive G1/s transitions in vascular smooth muscle cells. Circ Res. 2006; 98:1273–1281. [PubMed: 16627785]

Choi J, Husain M. Calmodulin-mediated cell cycle regulation: new mechanisms for old observations. Cell Cycle. 2006; 5:2183–2186. [PubMed: 16969097]

Diehl JA, Zindy F, Sherr CJ. Inhibition of cyclin D1 phosphorylation on threonine-286 prevents its rapid degradation via the ubiquitin-proteasome pathway. Genes & Development. 1997; 11:957–972. [PubMed: 9136925]

Duan Y, He X, Yang H, Ji Y, Tao T, Chen J, et al. Cyclin D3/CDK11(p58) complex involved in Schwann cells proliferation repression caused by lipopolysaccharide. Inflammation. 2010; 33:189–199. [PubMed: 20066559]

Fang MZ, Lee MH, Lee YS, Kim YC, Lee BM, Cho MH. Low expression of cyclin D2 in G2/M-arrested and transformed proliferating Balb/3T3 cells. J Vet Med Sci. 2002; 64:201–205. [PubMed: 11999438]

Gautschi O, Ratschiller D, Gugger M, Betticher DC, Heighway J. Cyclin D1 in non-small cell lung cancer: a key driver of malignant transformation. Lung Cancer. 2007; 55:1–14. [PubMed: 17070615]

Glover DM, Leibowitz MH, McLean DA, Parry H. Mutations in aurora prevent centrosome separation leading to the formation of monopolar spindles. Cell. 1995; 81:95–105. [PubMed: 7720077]

Hansen DV, Loktev AV, Ban KH, Jackson PK. Plk1 regulates activation of the anaphase promoting complex by phosphorylating and triggering SCFbetaTrCP-dependent destruction of the APC Inhibitor Emi1. Mol Biol Cell. 2004; 15:5623–5634. [PubMed: 15469984]

Hochstrasser M. Biochemistry. All in the ubiquitin family. Science. 2000; 289:563–564. [PubMed: 10939967]

Hu D, Valentine M, Kidd VJ, Lahti JM. CDK11(p58) is required for the maintenance of sister chromatid cohesion. J Cell Sci. 2007; 120:2424–2434. [PubMed: 17606997]

Ilyin GP, Rialland M, Glaise D, Guguen-Guillouzo C. Identification of a novel Skp2-like mammalian protein containing F-box and leucine-rich repeats. FEBS Lett. 1999; 459:75–79. [PubMed: 10508920]

Kahl CR, Means AR. Regulation of cell cycle progression by calcium/calmodulin-dependent pathways. Endocr Rev. 2003; 24:719–736. [PubMed: 14671000]

Korkotian E, Segal M. Lasting effects of glutamate on nuclear calcium concentration in cultured rat hippocampal neurons: regulation by calcium stores. J Physiol. 1996; 496(Pt 1):39–48. [PubMed: 8910194]

Lew DJ, Dulic V, Reed SI. Isolation of three novel human cyclins by rescue of G1 cyclin (Cln) function in yeast. Cell. 1991; 66:1197–1206. [PubMed: 1833066]

Lin DI, Barbash O, Kumar KG, Weber JD, Harper JW, Klein-Szanto AJ, et al. Phosphorylationdependent ubiquitination of cyclin D1 by the SCF(FBX4-alphaB crystallin) complex. Mol Cell. 2006; 24:355–366. [PubMed: 17081987]

Liu C, Kato Y, Zhang Z, Do VM, Yankner BA, He X. beta-Trcp couples beta-catenin phosphorylation-degradation and regulates Xenopus axis formation. Proc Natl Acad Sci U S A. 1999; 96:6273–6278. [PubMed: 10339577]

Lu KP, Rasmussen CD, May GS, Means AR. Cooperative regulation of cell proliferation by calcium and calmodulin in Aspergillus nidulans. Mol Endocrinol. 1992; 6:365–374. [PubMed: 1584213]

Malard V, Berenguer F, Prat O, Ruat S, Steinmetz G, Quemeneur E. Global gene expression profiling in human lung cells exposed to cobalt. BMC Genomics. 2007; 8:147. [PubMed: 17553155]

Mallampalli RK, Ryan AJ, Salome RG, Jackowski S. Tumor necrosis factor-alpha inhibits expression of CTP:phosphocholine cytidylyltransferase. J Biol Chem. 2000; 275:9699–9708. [PubMed: 10734122]

Myung SJ, Rerko RM, Yan M, Platzer P, Guda K, Dotson A, et al. 15-Hydroxyprostaglandin dehydrogenase is an in vivo suppressor of colon tumorigenesis. Proc Natl Acad Sci U S A. 2006; 103:12098–12102. [PubMed: 16880406]

Ohtani K, DeGregori J, Nevins JR. Regulation of the cyclin E gene by transcription factor E2F1. Proc Natl Acad Sci U S A. 1995; 92:12146–12150. [PubMed: 8618861]

Okabe H, Lee SH, Phuchareon J, Albertson DG, McCormick F, Tetsu O. A critical role for FBXW8 and MAPK in cyclin D1 degradation and cancer cell proliferation. PLoS One. 2006; 1:e128. [PubMed: 17205132]

Papay J, Krenacs T, Moldvay J, Stelkovics E, Furak J, Molnar B, et al. Immunophenotypic profiling of nonsmall cell lung cancer progression using the tissue microarray approach. Appl Immunohistochem Mol Morphol. 2007; 15:19–30. [PubMed: 17536303]

Peeper DS, Upton TM, Ladha MH, Neuman E, Zalvide J, Bernards R, et al. Ras signalling linked to the cell-cycle machinery by the retinoblastoma protein. Nature. 1997; 386:177–181. [PubMed: 9062190]

Petretti C, Savoian M, Montembault E, Glover DM, Prigent C, Giet R. The PITSLRE/CDK11p58 protein kinase promotes centrosome maturation and bipolar spindle formation. EMBO Rep. 2006; 7:418–424. [PubMed: 16462731]

Pszczolkowski MA, Lee WS, Liu HP, Chiang AS. Glutamate-induced rise in cytosolic calcium concentration stimulates in vitro rates of juvenile hormone biosynthesis in corpus allatum of Diploptera punctata. Mol Cell Endocrinol. 1999; 158:163–171. [PubMed: 10630416]

Ray NB, Durairaj L, Chen BB, McVerry BJ, Ryan AJ, Donahoe M, et al. Dynamic regulation of cardiolipin by the lipid pump Atp8b1 determines the severity of lung injury in experimental pneumonia. Nat Med. 2010; 16:1120–1127. [PubMed: 20852622]

Resnitzky D, Reed SI. Different roles for cyclins D1 and E in regulation of the G1-to-S transition. Mol Cell Biol. 1995; 15:3463–3469. [PubMed: 7791752]

Rhoads AR, Friedberg F. Sequence motifs for calmodulin recognition. FASEB J. 1997; 11:331–340. [PubMed: 9141499]

Ridsdale R, Tseu I, Wang J, Post M. CTP:phosphocholine cytidylyltransferase alpha is a cytosolic protein in pulmonary epithelial cells and tissues. Journal of Biological Chemistry. 2001; 276:49148–49155. [PubMed: 11583989]

Rosario CO, Ko MA, Haffani YZ, Gladdy RA, Paderova J, Pollett A, et al. Plk4 is required for cytokinesis and maintenance of chromosomal stability. Proc Natl Acad Sci U S A. 2010; 107:6888–6893. [PubMed: 20348415]

Santra MK, Wajapeyee N, Green MR. F-box protein FBXO31 mediates cyclin D1 degradation to induce G1 arrest after DNA damage. Nature. 2009; 459:722–725. [PubMed: 19412162]

Shan J, Zhao W, Gu W. Suppression of cancer cell growth by promoting cyclin D1 degradation. Mol Cell. 2009; 36:469–476. [PubMed: 19917254]

Sicinska E, Aifantis I, Le Cam L, Swat W, Borowski C, Yu Q, et al. Requirement for cyclin D3 in lymphocyte development and T cell leukemias. Cancer Cell. 2003; 4:451–461. [PubMed: 14706337]

Skaar JR, Pagan JK, Pagano M. SnapShot: F box proteins I. Cell. 2009; 137:1160–1160. e1161. [PubMed: 19524517]

Sterlacci W, Fiegl M, Hilbe W, Jamnig H, Oberaigner W, Schmid T, et al. Deregulation of p27 and cyclin D1/D3 control over mitosis is associated with unfavorable prognosis in non-small cell lung

cancer, as determined in 405 operated patients. J Thorac Oncol. 2010; 5:1325–1336. [PubMed: 20631637]

Tanaka Y, Tanaka N, Saeki Y, Tanaka K, Murakami M, Hirano T, et al. c-Cbl-dependent monoubiquitination and lysosomal degradation of gp130. Mol Cell Biol. 2008; 28:4805–4818. [PubMed: 18519587]

Tanguay DA, Colarusso TP, Doughty C, Pavlovic-Ewers S, Rothstein TL, Chiles TC. Cutting edge: differential signaling requirements for activation of assembled cyclin D3-cdk4 complexes in B-1 and B-2 lymphocyte subsets. J Immunol. 2001; 166:4273–4277. [PubMed: 11254678]

Taules M, Rius E, Talaya D, Lopez-Girona A, Bachs O, Agell N. Calmodulin is essential for cyclin-dependent kinase 4 (Cdk4) activity and nuclear accumulation of cyclin D1-Cdk4 during G1. J Biol Chem. 1998; 273:33279–33286. [PubMed: 9837900]

Tsang WY, Spektor A, Luciano DJ, Indjeian VB, Chen Z, Salisbury JL, et al. CP110 cooperates with two calcium-binding proteins to regulate cytokinesis and genome stability. Mol Biol Cell. 2006; 17:3423–3434. [PubMed: 16760425]

Tyers M, Willems AR. One ring to rule a superfamily of E3 ubiquitin ligases. Science. 1999; 284:601, 603–604. [PubMed: 10328744]

Wang C, Gale M Jr. Keller BC, Huang H, Brown MS, Goldstein JL, et al. Identification of FBL2 as a geranylgeranylated cellular protein required for hepatitis C virus RNA replication. Mol Cell. 2005; 18:425–434. [PubMed: 15893726]

Watanabe N, Arai H, Iwasaki J, Shiina M, Ogata K, Hunter T, et al. Cyclin-dependent kinase (CDK) phosphorylation destabilizes somatic Wee1 via multiple pathways. Proc Natl Acad Sci U S A. 2005; 102:11663–11668. [PubMed: 16085715]

Weiderpass E. Lifestyle and cancer risk. J Prev Med Public Health. 2010; 43:459–471. [PubMed: 21139406]

Wikenheiser KA, Clark JC, Linnoila RI, Stahlman MT, Whitsett JA. Simian virus 40 large T antigen directed by transcriptional elements of the human surfactant protein C gene produces pulmonary adenocarcinomas in transgenic mice. Cancer Research. 1992; 52:5342–5352. [PubMed: 1394139]

Zhang Q, Tian L, Mansouri A, Korapati AL, Johnson TJ, Claret FX. Inducible expression of a degradation-resistant form of p27Kip1 causes growth arrest and apoptosis in breast cancer cells. FEBS Lett. 2005; 579:3932–3940. [PubMed: 15996662]

Zhang S, Cai M, Xu S, Chen S, Chen X, Chen C, et al. Interaction of p58(PITSLRE), a G2/M-specific protein kinase, with cyclin D3. J Biol Chem. 2002; 277:35314–35322. [PubMed: 12082095]

Zheng N, Schulman BA, Song L, Miller JJ, Jeffrey PD, Wang P, et al. Structure of the Cul1-Rbx1-Skp1-F boxSkp2 SCF ubiquitin ligase complex. Nature. 2002; 416:703–709. [PubMed: 11961546]

Zi X, Agarwal R. Silibinin decreases prostate-specific antigen with cell growth inhibition via G1 arrest, leading to differentiation of prostate carcinoma cells: implications for prostate cancer intervention. Proc Natl Acad Sci U S A. 1999; 96:7490–7495. [PubMed: 10377442]

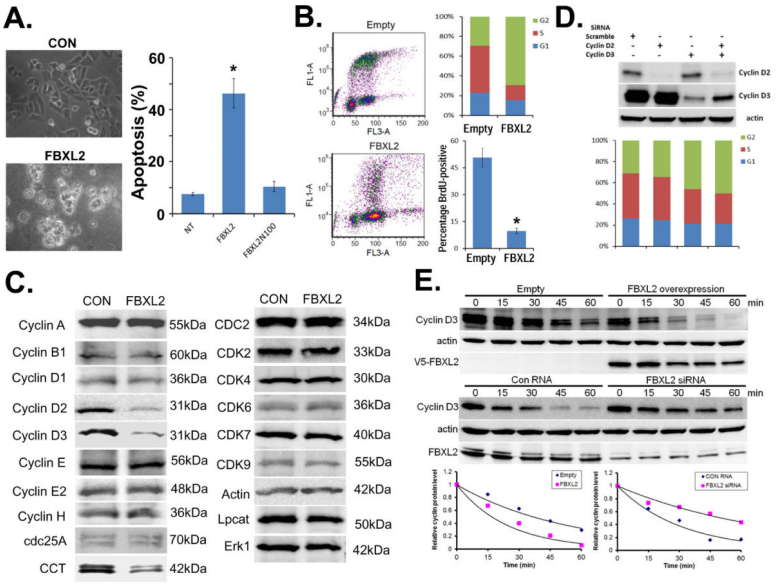

Figure 1. FBXL2 induces G2/M arrest via selective degradation of cyclins

A. MLE cells were transfected with either FBXL2 or mutant FBXL2 lacking the NH_2-terminal 100 residues. Cells were then observed under white field microscopy or assayed for ATP production. **B.** FACS analysis in MLE cells transfected with either an empty vector or FBXL2 plasmid (left panels, and upper right panel, *n=3*). DNA replication assay, monitored by BrdU incorporation (right lower panel, error bars indicate S.D.; *n*=3, *P<0.01). **C.** Immunoblotting showing levels of cyclins, CDKs, and negative control proteins, actin, Lpcat, and Erk, and a positive control protein (cytidylyltransferase, [CCT]), after control (CON) plasmid or ectopic FBXL2 expression. **D.** FACS analysis in cells transfected with scrambled RNA or siRNA to cyclin D2, cyclin D3, or both targets (lower panel). Immunoblotting of cells for cyclins and β-actin from lysates (upper panel). **E.** Cyclin D3 protein half-life determination after FBXL2 overexpression (**E**), or FBXL2 knockdown using siRNA (*n*=3 experiments). Below each panel levels of each protein on immunoblots were quantified densitometrically and shown graphically.

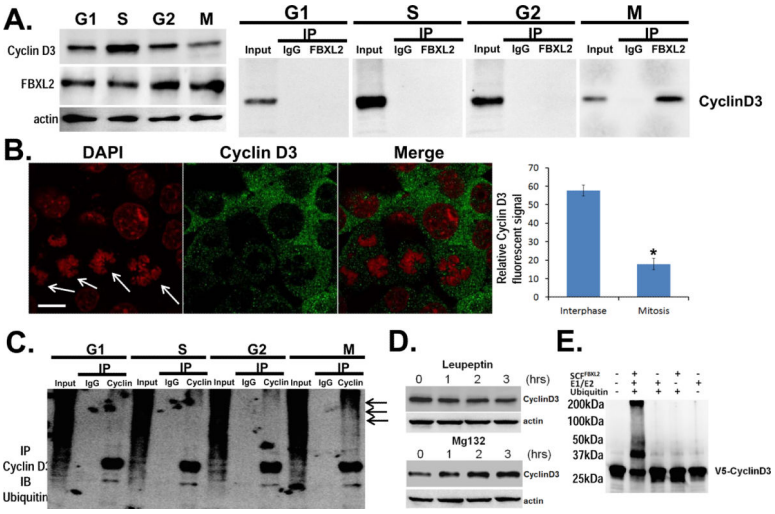

Figure 2. FBXL2 targets cyclin D3 for ubiquitination during mitosis

A. MLE cells were synchronized to each cell phase followed by co-immunoprecipitation of endogenous FBXL2 and then cyclin D3 immunoblotting. Shown on left are steady-state levels of cyclin D3, FBXL2, and actin in cell lysates. **B.** Cells were also immunostained for cyclin D3 and counterstained with DAPI to visualize nucleus. White arrows indicate at mitotic cells. Fluorescent intensity of endogenous cyclin D3 levels within cells at interphase versus cells undergoing mitosis was quantified using imageJ software and graphed on the right panel. **C**. *In vivo* ubiquitination assays. Polyubiquitinated cyclin D3 was detected by immunoprecipitation of endogenous cyclins followed by immunoblotting for ubiquitin. The arrows show polyubiquitinated cyclin D3. **D.** Cyclin D3 levels in cells treated with leupeptin or MG132. **E.** *In vitro* ubiquitination assays. Purified SCF complex components were incubated with V5-cyclin D3 and the full complement of ubiquitination reaction components (second lane from left) showing polyubiquitinated cyclin D3.

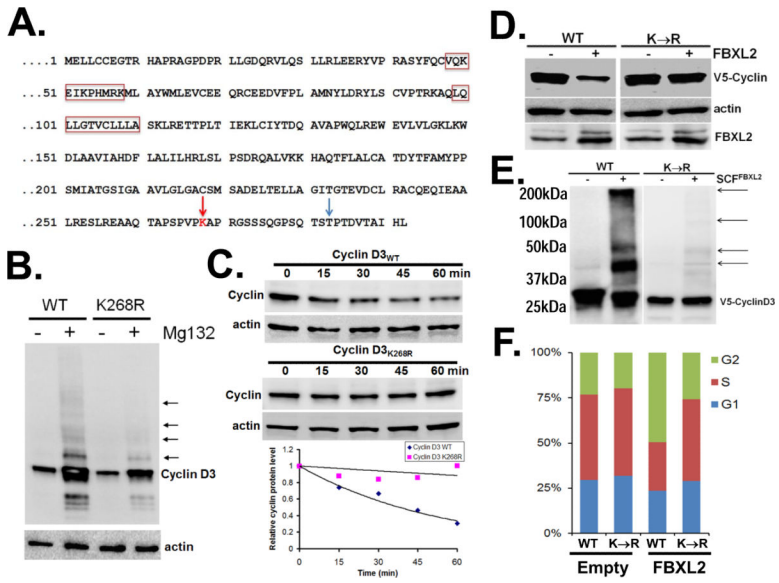

Figure 3. Cyclin D3 are polyubiquitinated at carboxyl-terminal acceptor sites

A. Primary sequence of cyclin D3. Red rectangle represents a potential IQ motif within cyclin D3. Red arrow indicates a potential ubiquitination site within cyclin D3. Blue arrow indicates a potential phosphorylation site within cyclin D3. **B.** Immunoblotting for accumulation of cyclin D3 wild type (WT) or point mutants in cells in the absence (−) or presence (+) of MG132 treatment. The arrows indicate lack of polyubiquitinated signals after expression of a Lys^{268R} cyclin D3 mutant. **C.** Cyclin D3 protein half-life determination after expression of WT V5-cyclin D3, or Lys^{268R} (V5-cyclin D3) mutant (data are from *n*=2 experiments). Below each panel levels of each protein on immunoblots were quantified densitometrically and shown graphically. **D.** Cyclin D3 protein levels in cells after co-transfection with either WT cyclin D3, or Lys^{268R} cyclin D3 with or without ectopic FBXL2 expression. **E.** *In vitro* ubiquitination assays. Purified SCF complex were incubated with WT V5-cyclin D3, or Lys^{268R} V5-cyclin D3 mutant and the full complement of ubiquitination reaction components. **F.** FACS analysis in cells prepared in **D (***n*=3 experiments).

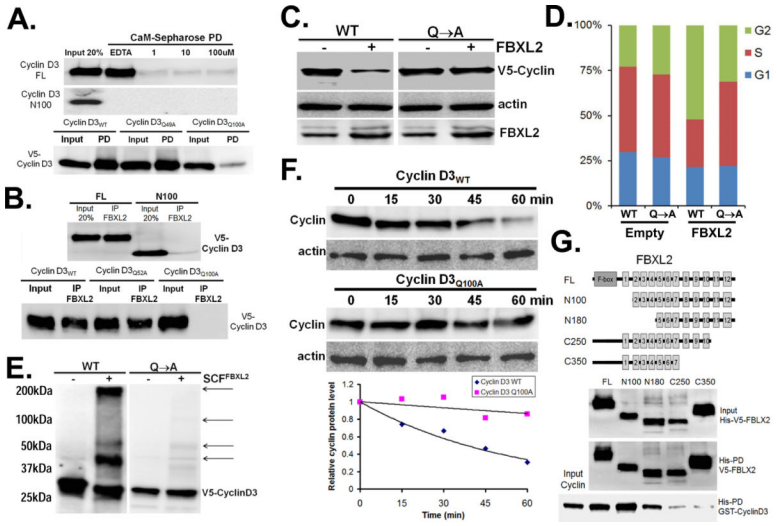

Figure 4. FBXL2 targets cyclin D3 within an IQ motif

A. CaM-sepharose pull-down (PD) assays showing effects of exogenous calcium on binding between CaM and either V5-full-length (FL) cyclins or V5-NH_2-terminal truncated (N100) mutants lacking the IQ motif within cyclin D3 (upper panel). CaM-sepharose pull-down assays showing levels of binding between CaM and WT cyclin D3 or D3 variants harboring point mutations within IQ motifs (lower panel). **B.** Coimmunoprecipitation of endogenous FBXL2 and V5-immunoblotting for FL or NH_2-terminal truncated (N100) mutant cyclin D3 (upper panel). Cells were transfected with V5-cyclin D3 variants harboring point mutations within IQ motifs followed by co-immunoprecipitation of endogenous FBXL2 and V5-immunoblotting (lower panel). **C−D.** Cells were co-transfected with WT cyclin D3 or a variant harboring a point mutation within the IQ motif with or without FBXL2 plasmid followed by immunoblotting for cyclins (left blot). **D**. Right: Cells were also analyzed by FACS, **(***n*=3 experiments). **E.** *In vitro* ubiquitination assays. Purified SCF complex were incubated with WT V5-cyclin D3, or an IQ motif point mutant, and the full complement of ubiquitination reaction components. **F.** Cyclin D3 protein half-life determination after expression of WT V5-cyclin D3, or an IQ motif point mutant (*n*=2 experiments). Below the panels levels of each protein on immunoblots were quantified densitometrically and shown graphically. **G.** Cell lysates expressing his-V5-FBXL2 truncation mutants (top, map) co-purified with GST-cyclin D3 using his-PD. After washing, proteins were eluted and processed for V5 or cyclin D3 immunoblotting.

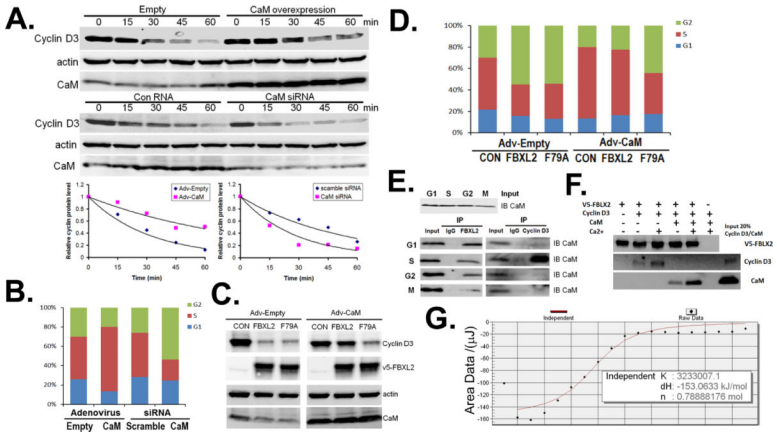

Figure 5. Calmodulin is an FBXL2 antagonist

A. Cyclin D3 protein half-life determination after adenoviral (Adv) CaM overexpression, or CaM knockdown using siRNA (*n*=2 experiments). Below each panel levels of each protein on immunoblots were quantified densitometrically and shown graphically. **B.** FACS analysis of cells after CaM overexpression or knockdown, (*n*=2 experiments). **C.** Levels of endogenous cyclin D3 protein in cells after co-expression of either Adv-empty, Adv-CaM, or WT FBXL2 or a FBXL2 mutant (F79A) that lacks ability to bind CaM. **D.** FACS analysis of cells prepared in **C**, (*n*=3 experiments). **E.** MLE cells were synchronized to each cell phase, followed by co-immunoprecipitation of endogenous FBXL2 or cyclin D3, and immunoblotting for CaM. Top immunoblot: input of CaM in total cell lysates prior to i.p. **F.** V5-FBXL2-agarose beads were generated and used as bait and incubated with combinations of purified GST-cyclin D3, or CaM with or without exogenous calcium. After washing of beads (150mM NaCl, 0.1% Triton X-100), proteins were eluted and resolved by SDS-PAGE followed by cyclin D3, CaM, and V5 immunoblotting. **G.** ITC binding analysis of CaM and peptide (LQLLGTVCLL) encoding a CaM-binding motif within cylicn D3 *in vitro*.

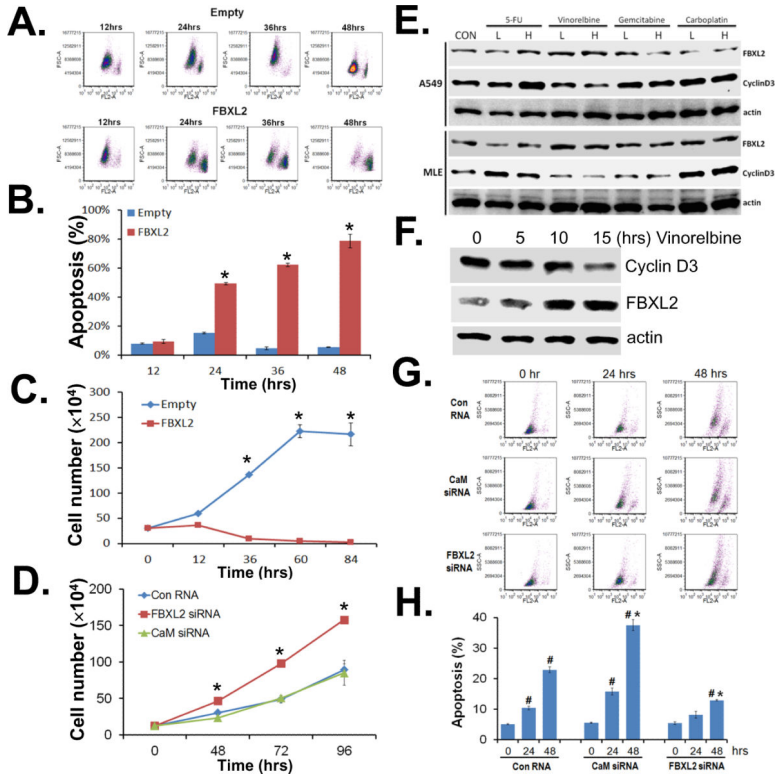

Figure 6. Ectopic expression of FBXL2 induces apoptosis

A–B. FACS analysis showing levels of apoptotic human adenocarcinoma (A549) cells after FBXL2 overexpression, (*n=3* experiments, **P*<0.01 versus empty). **C.** Proliferation studies of A549 cells after FBXL2 overexpression, (*n=3* experiments, **P*<0.01 versus FBXL2). **D.** Proliferation studies of A549 cells after FBXL2 or CaM knockdown (*n=3* experiments, **P*<0.05 versus control [CON]). **E.** A549 cells were treated with four chemotherapeutic agents using low (L) or high (H) concentrations. 18 h later, cells were collected, lysed, and immunoblotted with antibodies to the indicated proteins. **F.** FBXL2 and cyclin D3 immunoreactive levels after treatment with the chemotherapeutic agent vinorelbine. **G.** FACS analysis showing levels of apoptotic human adenocarcinoma (A549) cells after FBXL2 or CaM knockdown with vinorelbine treatment (*n=3* experiments, **P*<0.01 versus Con RNA, #*P*<0.01 versus 0 h). **H.** Data is quantated from FACS above.

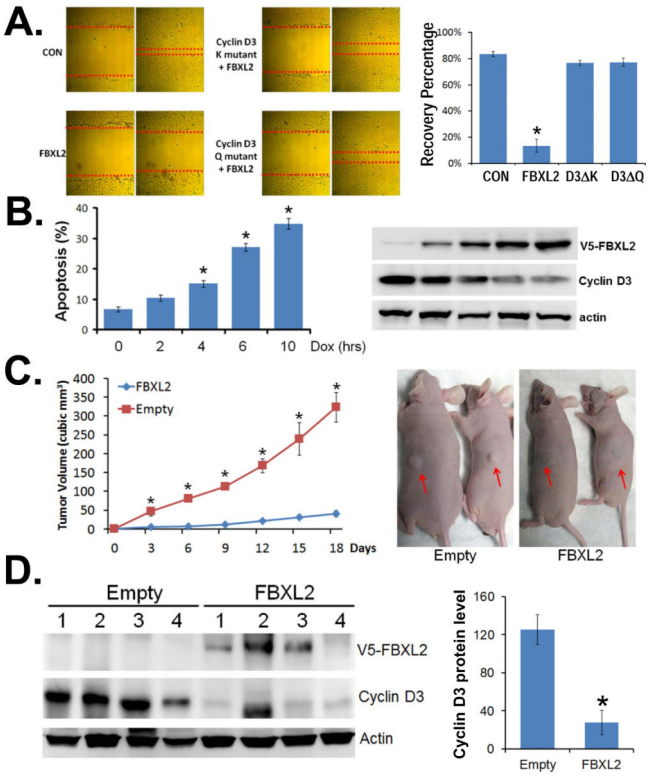

Figure 7. Ectopic FBXL2 expression inhibits tumor growth

A. Wound-healing assay. Confluent monolayers of A549 cells were injured and cellular migration into the wound was determined under control (CON) conditions, after FBXL2 overexpression (left panels), or after ectopic expression of cyclin D3 variants that harbor mutations within the ubiquitin acceptor site (K mutant, top right panel) or within the IQ motif (bottom right panel). Recovery of cells to wound heal was quatitated and graphed (right) **P*<0.01 versus other groups. **B.** FACS analysis showing levels of apoptotic A549 cells after doxycycline (Dox) inducible FBXL2 overexpression, (*n=3* experiments, **P*<0.05 versus 0 hr). The immunoblot on right shows levels of indicated proteins in cells. **C–D.** Effect of stable expression of FBXL2 or a control vector (Empty) on growth of A549 tumor implants in nude mice, *n=8* mice/group. The upper left panel shows tumor volume over time and shown at right are representative images of variable sizes of xenografts in two nude mice (arrows) after expression of an empty vector or FBXL2. For C, *n=8* mice/group **P*<0.05 versus FBXL2. In (D), tumors from four control and four FBXL2 treated A549 implants in mice were collected at the end-point, and assayed for cyclin D3 and FBXL2 proteins by immunoblotting. The right bar graph shows the denistometric data from immunoblots, **P*<0.05 versus empty.

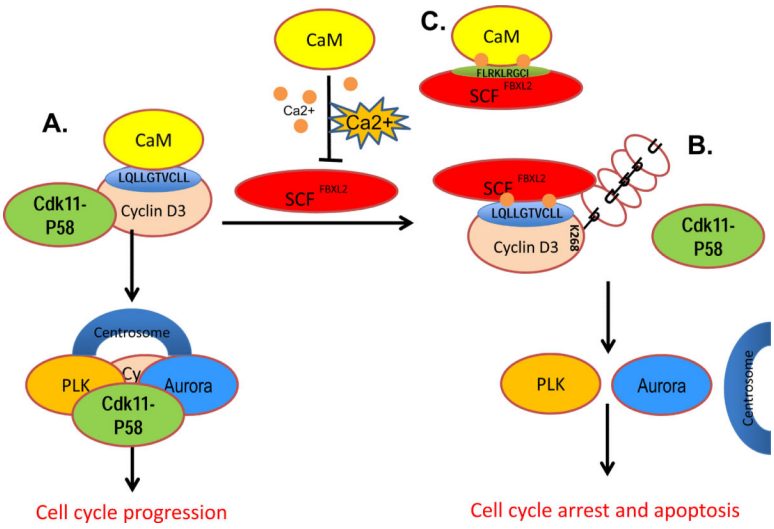

Figure 8. FBXL2 induction of cell cycle arrest is opposed by CaM

A. Calmodulin (CaM) binds within an IQ signature to protect cyclin D3 from SCF^{FBXL2}. This interaction is calcium independent and preserves cyclin D3 interaction with Cdk11p58 that promotes mitosis by recruitment of PLK4 and Aurora A to the centrosomes (bottom, left). **B**. Increases in calcium promotes SCF^{FBXL2} competing with CaM for IQ motif binding within cyclin D3 to mediate cyclin D3 polyubiquitination and subsequent degradation compromising its association with and activity of CDk11p58, essential for cell cycle progression. This process dislocates PLK4 and Aurora A from the centrosome, resulting in cell cycle arrest. **C**. In addition to competition for cyclin D IQ motif binding, CaM directly binds and antagonizes SCF^{FBXL2}.